Multi-Electron-Acceptor Dyad and Triad Systems Based on Perylene Bisimides and Fullerenes

Thomas W. Chamberlain, E. Stephen Davies, Andrei N. Khlobystov,* and Neil R. Champness*[a]

Abstract: Fullerene (C_{60}) and 3,4,9,10-perylene tetracarboxylic diimide (PTDCI) were used as building blocks for an electron acceptor dyad (C_{60}–PTCDI) and triad (C_{60}–PTCDI–C_{60}). As the first reduction potentials for C_{60} and PTCDI are very close, simultaneous introduction of two or three electrons is possible into the dyad and triad, respectively. Further stepwise electrochemical reduction leads to formation of a series of well-defined anionic species in which electrons associated with the fullerene or the PTDCI components of the molecule can be clearly distinguished. In total, up to four electrons can be reversibly injected into the dyad C_{60}–PTCDI and up to six into the triad C_{60}–PTCDI–C_{60} system. The optical absorption properties in the UV/Vis range are also crucially defined by the distribution of electrons between the acceptor parts, as the injection/removal of electrons causes drastic colour changes in the dyad and the triad systems.

Keywords: cyclic voltammetry · EPR spectroscopy · fullerenes · perylene bisimides · UV/Vis spectroscopy

Introduction

Molecules comprising electron-donor and electron-acceptor components and possessing light-absorbing properties are currently attracting significant attention in the context of photovoltaic devices and photocatalysis applications.[1–3] Distribution of photo- or electrochemically generated electrons in donor–acceptor dyads is usually predictable due to the significant differences between redox potentials for the donor and acceptor components. However, when two-electron-acceptor parts with similar redox potentials are combined within the same dyad, the location of incoming electrons is more difficult to predict as the two acceptors are competing for the electrons.[4] As a result, each part of the acceptor–acceptor dyad may accommodate an unpaired electron, giving rise to species with a high total electron spin, important for molecular electronic and magnetic applications.[5,6] Unpaired electrons residing on such a dyad will be spatially separated by a bridge linking its constituent parts. Since the separating distance is dictated by the length of that bridge, the strength of spin–spin interactions between

unpaired electrons can be controlled through the structure of the dyad. Such tunable multi-electron molecular systems in which information can be stored and processed in a form of electron spins have been considered as candidate materials for quantum information processing.[7]

In this study we have investigated acceptor–acceptor molecular systems based on fullerene (C_{60}) and 3,4,9,10-perylene tetracarboxylic diimide (PTCDI) derivatives. Both fullerenes and PTCDI-based species are an attractive target in forming multi-component acceptor–donor systems due to their extensive redox chemistry and photochemical properties.[4,8–14] Fullerene absorbs light in the UV/Vis range[2] and PTCDI strongly absorbs light in the Vis/near IR range,[15,16] and both possess excellent electron-acceptor characteristics[17–19] and have been identified as candidates for the development of photovoltaic devices.[20–22] For such applications it is imperative that the electronic/redox and optical properties of the molecular species are fully understood.

Fullerene cages appended at the "bay region" (1-, 6-, 7- and/or 12-positions) of the perylene core play the role of redox active sites capable of accommodating up to six electrons. Considering that any chemical functionalisation of fullerene cages introduces sp³-carbon atoms within the bridge linking PTCDI and C_{60}, no orbital overlap between the two moieties is expected. As a result, we demonstrate that the empty orbitals of pendant fullerene groups and the perylene core (designated as "LUMOs" to emphasise the fact that they are localised either on the C_{60} or PTCDI part of the dyad) are capable of accommodating electrons independently of each other. This enables reversible electrochemical switching of the fullerene–perylene conjugate molecules to polyanionic states, possessing up to three spatially

[a] Dr. T. W. Chamberlain, Dr. E. S. Davies, Dr. A. N. Khlobystov, Prof. N. R. Champness
School of Chemistry, University of Nottingham
University Park, Nottingham, NG7 2RD (UK)
Fax: (+44)115-95-13555
E-mail: Andrei.Khlobystov@notttingham.ac.uk
   Neil.Champness@nottingham.ac.uk

separated unpaired electrons and some interesting optical properties.

There are a small number of previous studies of PTCDI–fullerene species.[11–14] The majority of these studies differ significantly from our study in that the fullerene moiety is attached to the PTCDI group by means of the imide nitrogen.[11–13] Molecular orbital calculations on PTCDI derivatives reveal a node in the HOMO at the nitrogen atoms of the imide functions, precluding electronic communication pathways between imide appendages and the fullerene.[23] Of additional importance is the group used to functionalise the fullerene moiety. Previous studies have exploited either a cyclopropyl[11,12] or pyrrolidine coupling,[13,14] the former of which has been demonstrated to be unstable in some instances upon electrochemical reduction.[24] By exploiting pyrrolidine coupling at the fullerene and "bay region", PTCDI functionalisation should lead to the most chemical and electrochemically robust PTCDI derivatives and hence to the formation of stable acceptor–acceptor arrays. Although an extensive and elegant photophysical study of a

related system has been reported for a fullerene–PTCDI–porphyrin triad system,[14] there have not been extensive combined electrochemical/spectroelectrochemical/EPR studies of the multiple redox states of such systems.

Results and Discussion

Fullerene-perylene compounds **2** and **4** were prepared as outlined in Schemes 1 and 2, respectively. Following the ini-
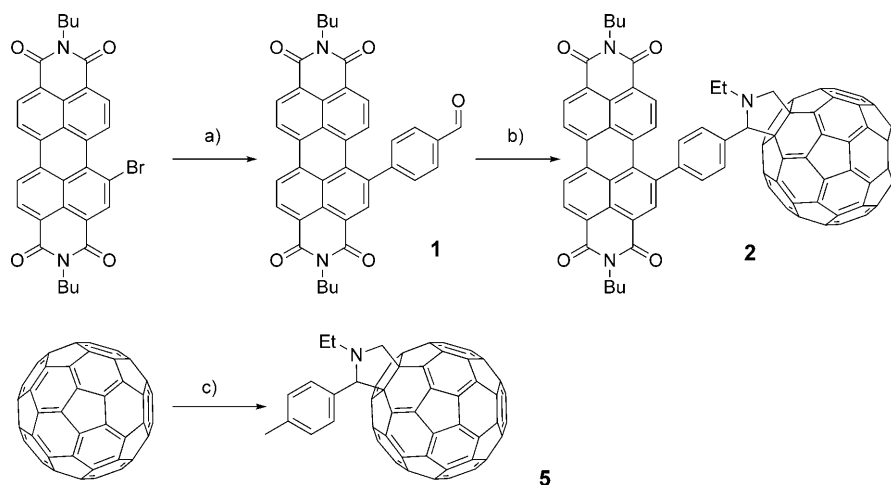
Scheme 1. Synthetic procedures for **1**, **2** and **5**. a) 4-boronic acid benzaldehyde, CsF, Ag₂O, Pd(PPh₃)₄, THF, 66 °C, 78 %; b) C₆₀, Et-NHCH₂COOH, toluene, 110 °C, 42 %; c) *p*-tolualdehyde, Et-NHCH₂COOH, toluene, 110 °C, 56 %.
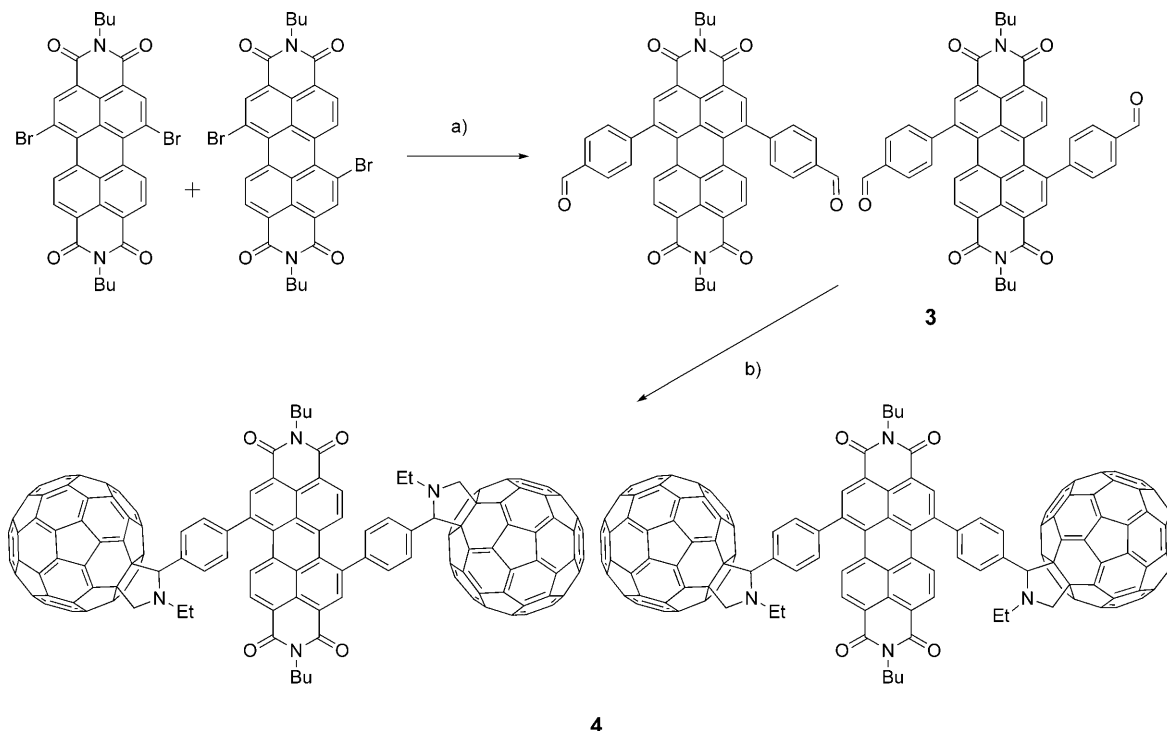
Scheme 2. Synthetic procedures for **3** and **4**. a) 4-boronic acid benzaldehyde, CsF, Ag₂O, Pd(PPh₃)₄, THF, 66 °C, 64 %; b) C₆₀, Et-NHCH₂COOH, toluene, 110 °C, 18 %. A mixture of both 1,7- and 1,6-Br₂–PTCDI were used in reaction a) and the resultant isomers of **3** were reacted further in reaction b).

tial introduction of bromine substituents to the perylene-tetracarboxylic acid core,[25] the aldehyde functionality of the intermediate compounds **1** and **3** were introduced by the Suzuki coupling of the mono-/bis-(bromo)-substituted perylenes with 4-boronic acid benzaldehyde.[26] The [3+2] cycloaddition of the azomethine ylide, formed by the addition of *N*-ethylglycine to the aldehyde intermediate, to one or two equivalents of C_{60} resulted in the formation of the five-membered pyrrolidine ring containing products **2** and **4** in good yields.[27] As discussed above a pyrrolidine linker was selected to functionalise the C_{60} moiety due to the enhanced stability of this linker to reduction in comparison to cyclopropyl linkers.[24]

In the case of compound **4** preparation of the dibromo-substituted PTCDI, *N,N'*-bis(*n*-butyl)dibromo-3,4,9,10-perylenetetracarboxylic bisimide, yields a mixture of both 1,7 and 1,6 isomers in an estimated 80:20 ratio, which it has not proven possible to separate.[28] The 1,7 isomer is always the major product from the bromination of perylene-3,4,9,10-tetracarboxylic acid and as a result the same isomer is also the major product from substitution reactions using the "as-synthesised" *N,N'*-bis(*n*-alkyl)dibromo-3,4,9,10-perylenetetracarboxylic bisimide. Thus in this study a small quantity of the 1,6 isomer is present in the final product, **4** (approximately 10% by ¹H NMR spectroscopy) used for all characterisation methods. Compound **5** {1,2-(1-ethyl-2-(4-methyl-benzene)-pyrrolidine)[60]fullerene}, was prepared by the [3+2] cycloaddition of C_{60} with *p*-tolualdehyde and *N*-ethyl-glycine and was used as a reference molecule for the fullerene moiety in the fullerene–perylene compounds.

Electrochemical studies: Since both fullerene and perylene moieties in compounds **2** and **4** are efficient electron acceptors with similar reduction potentials, determining the distribution of electrons in reduced forms of these molecules $[\mathbf{2}]^{n-}$ and $[\mathbf{4}]^{n-}$ is a challenging task that can be only achieved by the careful comparison of the redox and spectroscopic properties of these compounds with those of their corresponding reference compounds; **1** and **3** representing perylene moieties in **2** and **4**, respectively and **5** representing the fullerene moiety in both **2** and **4**. Results from cyclic voltammetry (CV) measurements of **1**–**5** are given in Table 1 and Figure 1. The results confirm that the first reductions of **2** and **4** involve the PTCDI moiety. It is worth noting that the shift in potential of the first reduction associated with the mono- and di-C_{60}-substituted compounds, **2** (−1.03 V) and **4** (−1.14 V), respectively, indicates that attachment of C_{60} groups increases electronic density in the PTDCI core.

Table 1. Redox potentials (CV) of C_{60}–PTCDI derivatives **2** and **4**, PTCDI derivatives **1** and **3** and C_{60} derivative **5**.[a]

	E_{1st}^{red}	E_{2nd}^{red}	E_{3rd}^{red}	E_{4th}^{red}	$\Delta E_{Fc+/Fc}$
1	−0.96 (0.08)	−1.15 (0.08)			0.08
	−0.96	*−1.14*			
2	−1.03 (0.11)[b]	−1.16 (0.07)[c]	−1.43 (0.06)[d]	−1.98 (0.07)[d]	0.07
	−1.03	*−1.17*	*−1.43*	*−1.98*	
3	−0.93 (0.09)	−1.12 (0.09)			0.07
	−0.92	*−1.11*			
4	−1.13 (0.14)[b]	−1.29 (0.08)[c]	−1.50 (0.10)[d]	−2.06 (0.10)[d]	0.19
	−1.14	*−1.25*	*−1.48*	*−2.04*	
5	−1.06 (0.07)	−1.44 (0.07)	−1.98 (0.07)		0.07
	−1.05	*−1.44*	*−1.98*		

[a] All potentials reported as $E_{1/2}$ ($= (E_p^a + E_p^c)/2$) in V vs. Fc⁺/Fc and quoted to the nearest 0.01 V; the values in brackets are ($E_p^a - E_p^c$) for couples; glassy carbon electrode as the working electrode; **1**, **2**, **3** and **5** in CH_2Cl_2 containing 0.4 M [NBu₄][BF₄]; **4** in 1,2-dichlorobenzene containing 0.4 M [NBu₄][BF₄]; scan rate = 100 mVs⁻¹. Values in italics taken from square wave voltammetry. [b] Reduction potentials associated with combined fullerene + perylene reductions. [c] Reduction potentials associated with perylene reduction. [d] Reduction potentials associated with fullerene reduction.
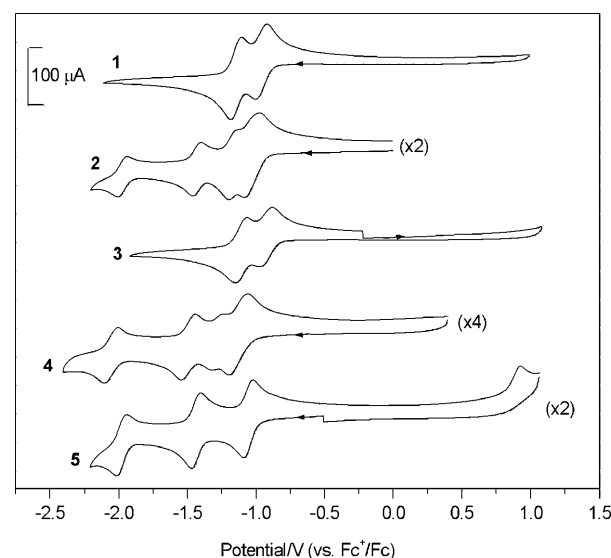

Figure 1. Cyclic voltammograms recorded for **1**, **2**, **3** and **5** in CH_2Cl_2 containing [Bu₄N][BF₄] (0.4 M) and for **4** in 1,2-dichlorobenzene containing [Bu₄N][BF₄] (0.4 M). Results of square wave voltammetry studies are presented in Figure S1 in the Supporting Information.

Conversely, the first reductions for reference compounds **1** (−0.96 V) and **3** (−0.92 V) demonstrate that the phenylaldehyde group(s) withdraw electron density from the PTCDI core leading to more facile first reductions than for simpler phenyl-substituted analogues.[28]

Hence, from these results it was anticipated that the appendage of one C_{60}–PTCDI (**2**) or two C_{60}–PTCDI–C_{60} (**4**) fullerene cages to the perylene core would result in the overlap of first reductions on the PTCDI and C_{60} moieties and as a consequence increase the electron uptake to four for **2** (two electrons each from PTCDI and C_{60} components) or six for **4** (two electrons from PTCDI and four electrons from the two C_{60} components) in the 0 to −1.5 V range of potentials (Figure 1, Table 1 and Figure S1 in the Supporting Information file). In agreement with this, the CV of **2** and **4**

gave an overlap of the first reduction potentials of the fullerene and perylene moieties allowing **2** and **4** to accept more than one electron in the initial reduction step. Quantitative analysis by coulometry shows simultaneous reduction of C_{60} and PTDCI moieties in **2** and **4** (Figure 1) that converts them to $[2]^{2-}$ and $[4]^{3-}$ species at potentials corresponding to the first reduction process (-1.03 V and -1.14 V, respectively). Taking into account the redox potentials of the reference compounds (Table 1), distribution of electrons in $[2]^{2-}$ should be expected as $C_{60}{}^{•-}$–PTCDI$^{•-}$ and in $[4]^{3-}$ as $C_{60}{}^{•-}$–PTCDI$^{•-}$–$C_{60}{}^{•-}$. This hypothesis was confirmed by the results of UV/Vis spectroelectrochemical studies discussed below.

UV/Vis spectroelectrochemical studies: The UV/Vis spectroelectrochemical data for compounds **1**–**5** in neutral and reduced states are given in Table 2. Both the PTCDI and

Table 2. UV/Vis spectroelectrochemical data for compounds **1**–**5** in neutral and reduced states.

	λ_{max} [nm] ($\varepsilon \times 10^{-4}$ [mol^{-1} m^3 cm^{-1}])
[**1**]	262 (3.5), 323 (1.4), 379 (0.4), 498 (2.9), 534 (4.2)
[**1**]$^-$	235 (5.3), 326 (1.0), 355 (0.7), 378 (0.7), 404 (0.7), 490 (0.3), 542 (0.3), 721 (6.1), 809 (3.1)
[**1**]$^{2-}$	231 (4.6), 277 (4.8), 398 (0.7), 435 (0.9), 588 (5.7)
[**2**]	244 (8.9), 328 (2.9), 430 (0.7), 506 (1.8), 539 (2.3)
[**2**]$^{2-}$	242 (10.0), 726 (4.4), 812 (2.1), 871 (0.8)
[**2**]$^{3-}$	262 (8.7), 579 (4.3), 602 (3.7), 643 (1.9)
[**2**]$^{4-}$	267 (8.5), 579 (4.4), 601 (3.9), 642 (2.0), 709 (0.5), 867 (0.6)
[**3**]	261 (3.6), 322 (2.3), 391 (0.4), 543 (2.6)
[**3**]$^-$	235 (4.5), 265 (4.1), 356 (0.9), 378 (0.9), 418 (0.9), 492 (0.4), 526 (0.4), 733 (0.4), 822 (2.0), 876 (1.0)
[**3**]$^{2-}$	230 (4.1), 279 (4.9), 406 (1.0), 602 (4.5)
[**4**]	432 (0.5), 562 (0.8)
[**4**]$^{3-}$	750 (1.6), 835 (0.8)
[**4**]$^{4-}$	595 (1.6), 621 (1.8), 653 (1.1)
[**4**]$^{6-}$	595 (1.7), 621 (1.9), 652 (1.2), 867 (0.4)
[**5**]	256 (6.3), 306 (2.0), 325 (1.9), 430 (0.2)
[**5**]$^-$	263 (5.6), 766 (0.2)
[**5**]$^{2-}$	266 (5.1), 721 (0.4), 863 (0.6)
[**5**]$^{3-}$	748 (0.4), 863 (0.5)

C_{60} parts of **2** (Figure 2) and **4** (Figure 3) absorb light in the UV/Vis range, which enables one to follow the addition of electrons into "LUMOs" of these molecules by optical spectroscopy. When correlated with the spectra of the reference compounds (see the Supporting Information), the optical absorption spectra of the fullerene–perylene conjugates appear as simple superpositions of fullerene and perylene spectra thus indicating little or no orbital overlap in the charge-neutral ground state of these molecules. As a result of the perylene chromophore having a significantly higher extinction coefficient than that of the fullerene, the spectra of **2** and **4** are dominated by the strong absorption bands of the PTCDI moiety masking the fullerene absorption bands; however, a characteristic band at 430 nm in reference compound **5** is evident in both **2** (430 nm) and **4** (432 nm). The $[2]^{2-}$ dianion formed at the first reduction step shows new absorbance bands including two very strong peaks at 726 and 812 nm (Figure 2), which clearly indicate that some of
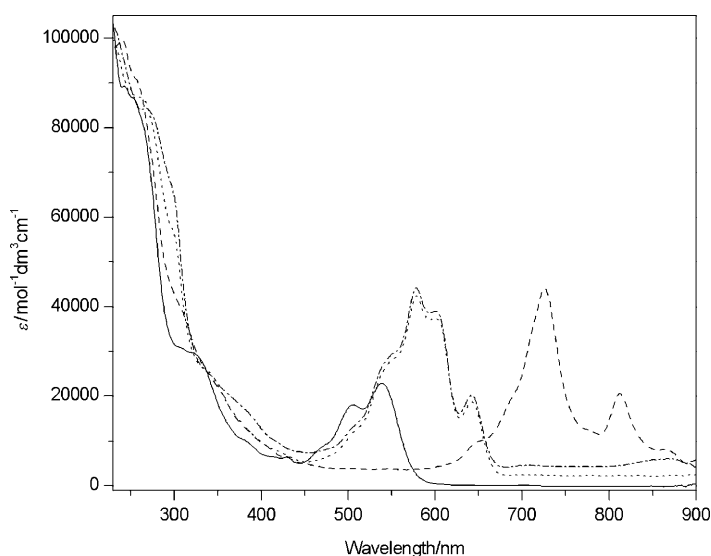

Figure 2. UV/Vis spectra recorded in CH_2Cl_2 containing $[Bu_4N][BF_4]$ (0.4 M) using spectroelectrochemical methods for **2** at 273 K; the spectrum of **2** is represented by the solid line, $[2]^{2-}$ (dashed line), $[2]^{3-}$ (dotted line) and $[2]^{4-}$ (dashed-dotted line).
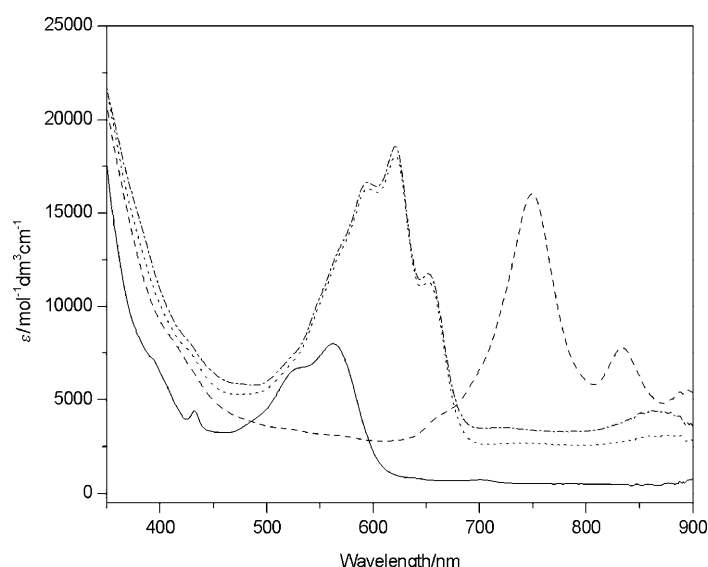

Figure 3. UV/Vis spectra recorded in 1,2-dichlorobenzene containing $[Bu_4N][BF_4]$ (0.2 M) using spectroelectrochemical methods for **4** at 273 K; the spectrum of **4** is represented by the solid line, $[4]^{3-}$ (dashed line), $[4]^{4-}$ (dotted line) and $[4]^{6-}$ (dashed-dotted line).

the electrons are located on the "LUMO" of the perylene part of **2**. Comparison with the spectra obtained for the reference perylene compound $[1]^-$ confirmed that only one electron resides on the PTCDI moiety in $[2]^{2-}$ (Figure S2, Supporting Information), and therefore the second electron should reside on the C_{60} part, so that $[2]^{2-}$ exists as a biradical dianion $C_{60}{}^{•-}$–PTCDI$^{•-}$. The state of **2** can be reversibly cycled between the C_{60}–PTCDI and $C_{60}{}^{•-}$–PTCDI$^{•-}$. A similar strategy applied to compound **4** showed that it undergoes a reduction to the trianion $[4]^{3-}$ (Figure 3); how-

ever, in contrast to compound **2**, reductions of **4** have not demonstrated complete chemically reversibility in the spectroelectrochemical cell. It was noted that no evident bands associated with decomposition were present and the lack of complete return of original spectra might result from the extended timescales that were required in order to achieve the various reduction levels under the conditions of this experiment. The profiles of species generated upon reduction of **4** were consistent with analogous reductions of **2**. According to optical spectroelectrochemical measurements [**4**]$^{3-}$ contains just one electron on its PTCDI moiety, and therefore, taking into account the large difference between the 1st and 2nd reduction potentials of the fullerene cage (Table 1), the trianion species should exist as a triradical $C_{60}^{\bullet-}$–PTCDI$^{\bullet-}$–$C_{60}^{\bullet-}$.

Radical anions [**2**]$^{2-}$ and [**4**]$^{3-}$ have one electron per each of their "LUMOs", and therefore addition of any further electrons will result in the pairing of incoming electrons with those already present in the molecules. Formation of [**2**]$^{3-}$ is accompanied by the disappearance of the strong absorption bands at 726 and 812 nm associated with the single-electron-doped perylene core and the emergence of a new set of bands at 579, 602 and 643 nm (Figure 2) consistent with two electrons on the perylene "LUMO" (c.f. [**1**]$^{2-}$, Figure S2, Supporting Information). Therefore the electron distribution in the [**2**]$^{3-}$ radical trianion is described as $C_{60}^{\bullet-}$–PTCDI^{2-}. The optical spectrum of [**2**]$^{4-}$ is very similar to that of trianion [**2**]$^{3-}$, indicating no changes in the state of the perylene core; however, an additional broad feature is developed at low energy (867 nm) that is consistent with a band for C_{60}^{2-} in [**5**]$^{2-}$ (at 863 nm), so that the electron distribution in [**2**]$^{4-}$ can be described as C_{60}^{2-}–PTCDI^{2-}. The anions [**2**]$^{3-}$ and [**2**]$^{4-}$ can be interconverted reversibly; hence compound **2** can be reversibly switched between C_{60}–PTCDI, $C_{60}^{\bullet-}$–PTCDI$^{\bullet-}$, $C_{60}^{\bullet-}$–PTCDI^{2-} and C_{60}^{2-}–PTCDI^{2-} levels.

The absorption spectrum of [**4**]$^{4-}$ (Figure 3) clearly indicates that the "LUMO" of perylene moiety is populated with two paired electrons (PTCDI^{2-}), which means that each of the fullerene cages will have an unpaired electron, so that the electron distribution in [**4**]$^{4-}$ can be expressed as $C_{60}^{\bullet-}$–PTCDI^{2-}–$C_{60}^{\bullet-}$. Similar to the transition between [**2**]$^{3-}$ and [**2**]$^{4-}$, the optical spectrum of [**4**]$^{6-}$ is very similar to that of tetraanion [**4**]$^{4-}$ indicating no changes in the state of the perylene core; however, an additional broad feature is developed at low energy (867 nm) that is consistent with a band for C_{60}^{2-} in [**5**]$^{2-}$ (at 863 nm), so that the electron distribution in [**4**]$^{6-}$ can be described as C_{60}^{2-}–PTCDI^{2-}–C_{60}^{2-}.

EPR spectroscopic studies: The results from spectroelectrochemical studies have given an insight into the nature of the molecular orbital into which the electron is added for the C_{60}–PTCDI conjugates at stages in the reduction sequence, this is now extended to the investigation of how these electrons interact when in these orbitals.

Coulometry has allowed us the control of the number of electrons added per molecule (**1**–**5**) in solution so that the

various reduced states have been generated and studied by electron paramagnetic resonance (EPR) spectroscopy. One-electron reduction of reference compounds **1**, **3** and **5** indicates that the position and shape of the EPR spectrum obtained from a single electron occupying either a fullerene- or a PTCDI-based "LUMO" was distinctly different (Figures S5–S8 in the Supporting Information). For PTCDI containing **1** and **3**, reduction to the monoanions [**1**]$^{-}$ and [**3**]$^{-}$, gives EPR active species with extensive hyperfine interactions and g_{iso} values of 2.0036 and 2.0034, respectively (Figure S5 and S7 in the Supporting Information). Subsequent reduction to the dianions, [**1**]$^{2-}$ and [**3**]$^{2-}$, results in a loss of EPR activity as the two electrons pair in the PTCDI orbital; hence only residual signals are recorded. For fullerene based **5**, reduction to the monoanion generates a paramagnetic species with $g_{iso} = 2.0003$, the signal of which is depleted upon reduction to [**5**]$^{2-}$ (Figure S8 in the Supporting Information).

Given that both **2** and **4** have two possible "LUMO" orbitals, and from the results of (spectro)electrochemical studies these are populated at the same or very similar potentials such that the first reduction should yield [**2**]$^{2-}$ and [**4**]$^{3-}$, respectively, we have attempted to sequentially reduce **2** to [**2**]$^{2-}$ and [**4**] to [**4**]$^{3-}$ by the addition of single equivalents of electrons in order to observe the distribution of these electrons in the system. However, the actual distribution of these electrons is determined by thermodynamic equilibria and as such we note the form of the CV (Figure 1) in each case. For **2** the first reduction results from an overlap of one electron reductions on both PTCDI and fullerene moieties. Thermodynamics would dictate that whilst we can add a single equivalent of electrons into **2**, these electrons could be distributed as $C_{60}^{\bullet-}$–PTCDI and C_{60}–PTCDI$^{\bullet-}$, or equilibrated as $C_{60}^{\bullet-}$–PTCDI$^{\bullet-}$ and C_{60}–PTCDI. Addition of a second equivalent of electrons should give $C_{60}^{\bullet-}$–PTCDI$^{\bullet-}$ only, as a dianion with two unpaired electrons and therefore this would have both singlet and triplet electronic states. We have estimated that the distance between spin distributions based on one on C_{60} and the other on PTCDI is 0.86–1.21 nm and at this relatively large separation the exchange interaction that separates the energies of the singlet and triplet states is expected to be less than 1 cm^{-1}. Therefore at room temperature both states should have similar populations and the $C_{60}^{\bullet-}$–PTCDI$^{\bullet-}$ dianion should be considered as a biradical.[30] A similar consideration can be made for **4** although the first reduction process is an overlap of two fullerene and one PTCDI reductions therefore the system is not locked to a single species in solution until $C_{60}^{\bullet-}$–PTCDI$^{\bullet-}$–$C_{60}^{\bullet-}$ is generated by the addition of three electrons (Scheme 3). At this point the EPR spectrum will result from the magnitude of interactions between three electrons, one in each separate "LUMO" of the triad. Reductions beyond [**2**]$^{2-}$ and [**4**]$^{3-}$ will result in the spin-pairing of electrons in these "LUMOs".

Addition of sub-two equivalents of electrons to a red solution of **2** (experimentally this was achieved in two ways, either by the addition of one equivalent of electrons to [**2**]
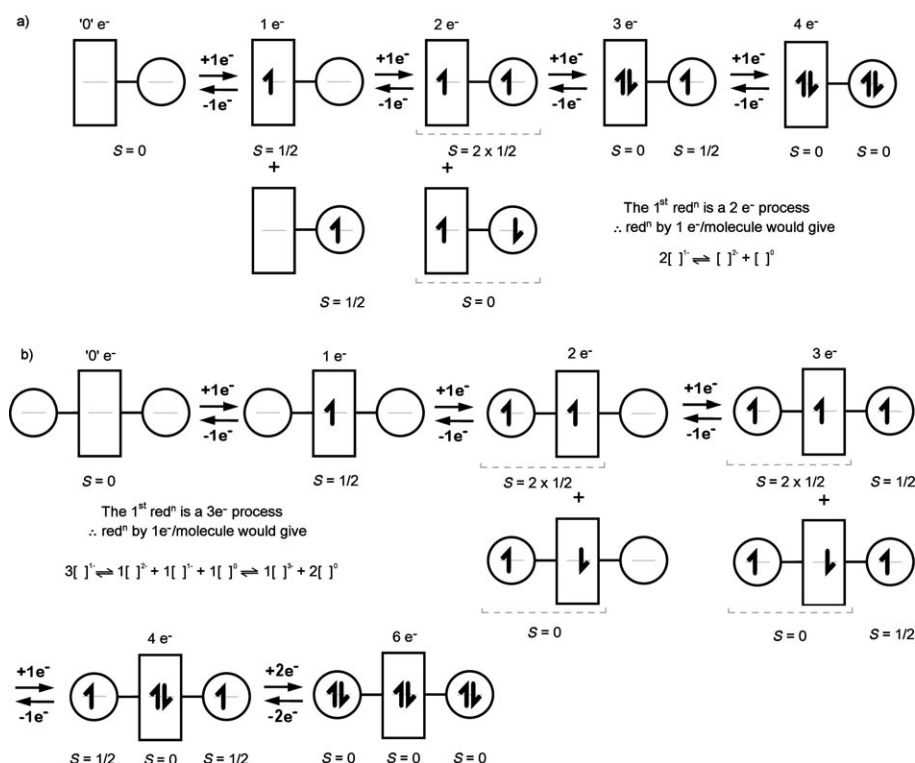
Scheme 3. Proposed electron configurations in the HOMOs of a) dyad $[2]^{n-}$ ($n=0$-4) and b) triad $[4]^{n-}$ ($n=0$–6) acceptor–acceptor systems. The individual PTCDI and fullerene units are represented by a rectangle and circle respectively. The unpaired electrons which interact strongly to generate a single signal in solution EPR are grouped with dashed lines.

The three-electron reduction of compound **4** to $[4]^{3-}$ can be similarly examined step by step using the bulk solution electrolysis technique coupled with EPR spectroscopy. The initial purple solution of **4** was electrolysed to give $[4]^{-}$ as a green solution. The EPR signal for $[4]^{-}$ has a g_{iso} value of about 2.003 and a very broad shape and as for $[2]^{-}$ ($g_{iso}=2.0032$) might indicate that the first electron is located in an orbital containing PTCDI character. Addition of a second and third equivalent of electrons leads to the formation of $[4]^{2-}$ and $[4]^{3-}$ as brown and green solutions, respectively. The addition of a second equivalent of electrons to $[4]^{-}$ resolves a signal with $g_{iso}=2.0014$ for $[4]^{2-}$ (Figure 6) that is very similar in shape and position to the broad signal noted for $[2]^{2-}$ at $g_{iso}=2.0018$ and on this basis we assign this signal to that of a biradical,
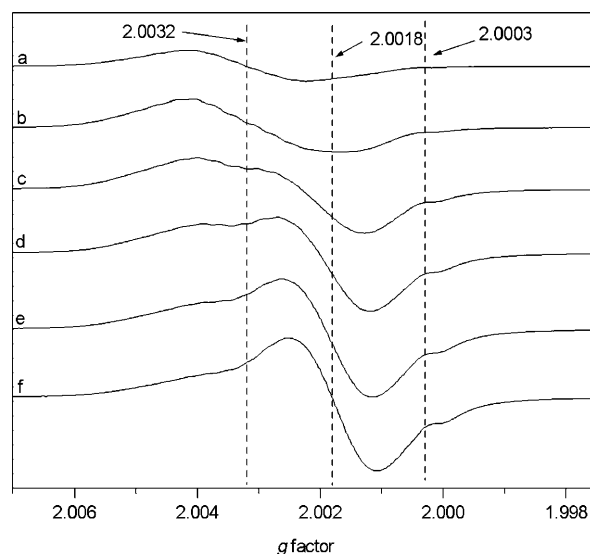
as in Figure S9 in the Supporting Information or in reverse by first generating $[2]^{2-}$ then allowing the slow re-oxidation of the sample as in Figure 4) resulted in the generation of a green solution, which is consistent with the formation of mono-anion based on PTCDI in each case. The main EPR signal of $[2]^{-}$ is relatively low in intensity (Figure 4a) and has a broad profile with $g_{iso}=2.0032$, suggesting that this represents an electron residing on a "LUMO" containing PTCDI character (the presence of hyperfine splitting is noted but not sufficiently resolved for analysis). From the results of optical measurements for $[2]^{2-}$ it would be expected that one electron occupies an orbital based on fullerene and the other occupies a PTCDI based orbital. Addition of electrons up to two equivalents leads to the formation of $[2]^{2-}$ (Figure 4 f) as a green/blue solution the EPR spectrum of which gives a signal at $g_{iso}=2.0018$. This value corresponds to an average g-value between $[2]^{-}$ (with an electron based on PTCDI; $g_{iso}=2.0032$) and $[5]^{-}$ (with an electron based on $C_{60}^{\bullet-}$; $g_{iso}=2.0003$). This is evidence for assignment of $[2]^{2-}$ as a biradical, with strong exchange coupling between the two unpaired electrons, in this case with one electron on PTCDI and the other on C_{60} in the $C_{60}^{\bullet-}$–PTCDI$^{\bullet-}$ dianion. The two smaller signals noted to higher and lower field of $g_{iso}=2.0018$ in Figure 4 f are attributed to the presence of $C_{60}^{\bullet-}$–PTCDI and C_{60}–PTCDI$^{\bullet-}$, respectively, resulting from slight re-oxidation of the sample during manipulation.

Figure 4. Experimental EPR spectra of $[2]^{n-}$ ($0<n\geq2$), Spectra a)–e) were obtained by the slow re-oxidation of $[2]^{2-}$, spectrum f) is $[2]^{2-}$. All spectra were recorded in CH_2Cl_2 containing $[Bu_4N][BF_4]$ (0.2 M) at ambient temperature. Analogous data recorded in 1,2-dichlorobenzene containing $[Bu_4N][BF_4]$ (0.2 M) for $[2]^{-}$, $[2]^{2-}$ and $[2]^{3-}$ are presented in Figure S9 in the Supporting Information.

analogous to $[2]^{2-}$, with strong exchange interaction between unpaired electrons on PTCDI and C_{60} in the $C_{60}^{\bullet-}$–PTCDI$^{\bullet-}$–C_{60} dianion. On acquisition of the third electron

the trianion $[4]^{3-}$ is formed and results from optical spectroscopic measurements suggest a $C_{60}^{\bullet-}$–PTCDI$^{\bullet-}$–$C_{60}^{\bullet-}$ distribution of electrons. The EPR spectrum of $[4]^{3-}$ retains the broad signal with $g_{iso}=2.0014$ assigned as the biradical of $[4]^{2-}$ and develops a signal at $g_{iso}=2.0004$; this is consistent with an unpaired electron on a fullerene cage. The lack of apparent perturbation of the biradical signal of $[4]^{2-}$ in the spectrum of $[4]^{3-}$ and the presence of a new C_{60} anion signal is not inconsistent with the presence of distinct (non-interacting) biradical and doublet states for $[4]^{3-}$.

From the results of UV/Vis spectroelectrochemistry the electron distribution in $[2]^{3-}$ is described as $C_{60}^{\bullet-}$–PTCDI^{2-} and this is supported by the results of EPR spectroscopy (Figure 5); the signal at $g_{iso}=2.0003$ is solely due to the un-
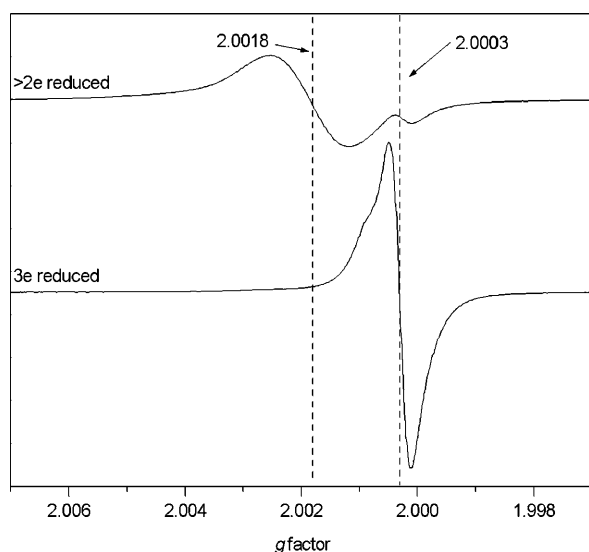

Figure 5. Experimental EPR spectra of $[2]^{2-}$ (upper trace) and $[2]^{3-}$ (lower trace). All spectra were collected in CH_2Cl_2 containing $[Bu_4N]$-$[BF_4]$ (0.2 M) at ambient temperature. The high field signal in the upper trace is attributed to a small quantity of $[2]^{3-}$ present in the sample as a result of slight over reduction.

paired electron present on the fullerene based "LUMO", since the shape and position of the EPR signal is almost identical to that of reference compound $[5]^-$ ($g_{iso}=2.0003$) (Figure S8 in the Supporting Information). The third electron enters the PTCDI orbital and spin-pairs with the electron already present (consistent with results of introducing a second electron in PTCDI models **1** and **3**) to give a system with a single unpaired electron on fullerene. The fourth electron added to **2** goes into the fullerene "LUMO" so that the two electrons present on the fullerene cage pair up leading to an effective quenching of EPR signal of tetraanion $[2]^{4-}$ relative to $[2]^{3-}$ (a residual signal comprising 12 % of the double integrated intensity of $[2]^{3-}$ is noted but has not been investigated further; Figure S10 in the Supporting Information) to give C_{60}^{2-}–PTCDI^{2-} and consistent with the results from the UV/Vis spectroscopy of $[2]^{4-}$.
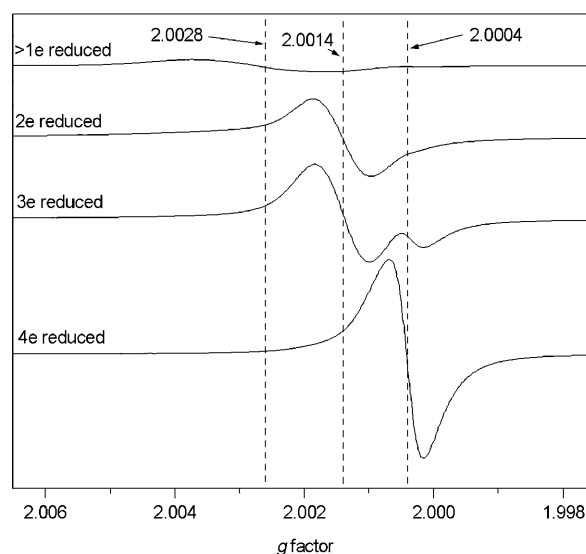

Figure 6. Experimental EPR spectra of $[4]^-$ (upper trace), $[4]^{2-}$, (upper middle trace), $[4]^{3-}$, (lower middle trace) and $[4]^{4-}$(lower trace). All spectra were collected in 1,2-dichlorobenzene containing $[Bu_4N][BF_4]$ (0.2 M) at ambient temperature.

The absorption spectrum of $[4]^{4-}$ (Figure 3) clearly indicates that the "LUMO" of perylene moiety is populated with two paired electrons (PTCDI^{2-}), which means that each of the fullerene cages will have an unpaired electron so that the electron distribution in $[4]^{4-}$ can be expressed as $C_{60}^{\bullet-}$–PTCDI^{2-}–$C_{60}^{\bullet-}$. EPR spectroscopy confirms that the two unpaired electrons are solely located on each of the fullerene "LUMO"s ($g_{iso}=2.0004$) and that their spins are essentially non-interacting in this biradical. It is worth noting that the intensity of the signal derived from the two unpaired electrons for the fullerene anions in $[4]^{4-}$ is considerably greater than that of the corresponding signal in $[4]^{3-}$, which was also anticipated to arise from the same two unpaired electrons on fullerene. This indicates a change in the observed electron coupling and is consistent with the loss of the biradical associated with the strong exchange interaction between one electron on a fullerene and one on PTCDI as a second electron is introduced into the PTCDI orbital. Hence $[4]^{4-}$ would represent a biradical in which the two unpaired electrons, one on each of the fullerenes, show a weak exchange interaction. The EPR spectrum of $[4]^{6-}$ showed that the hexaanion is essentially a diamagnetic species with all electrons paired (a residual signal comprising 11 % of the double integrated intensity of $[4]^{4-}$ is noted but not studied further; Figure S11 in the Supporting Information) hence each of the electrons added enters a fullerene based orbital and is spin-paired with the electron already present thus giving an electron distribution of C_{60}^{2-}–PTCDI^{2-}–C_{60}^{2-} and confirming the results of optical spectroscopic studies.

Conclusion

The comparison of electrochemical (CV and square wave voltammetry) and UV/Vis spectroelectrochemical data for **2** and **4** with that of their reference compounds (**1**, **3** and **5**) has allowed unambiguous assignment to the order of orbital population for $[2]^{2-}$, $[2]^{3-}$ and $[2]^{4-}$ as $C_{60}^{\bullet-}$–PTCDI$^{\bullet-}$, $C_{60}^{\bullet-}$–PTCDI^{2-} and C_{60}^{2-}–PTCDI^{2-}, respectively and for $[4]^{3-}$, $[4]^{4-}$ and $[4]^{6-}$ as $C_{60}^{\bullet-}$–PTCDI$^{\bullet-}$–C_{60}, $C_{60}^{\bullet-}$–PTCDI^{2-}–$C_{60}^{\bullet-}$ and C_{60}^{2-}–PTCDI^{2-}–C_{60}^{2-}, respectively.

Results from fluid solution EPR spectroscopic studies are equally unambiguous; $[2]^{2-}$ appears as a biradical with strong exchange interaction between unpaired electrons on PTCDI and C_{60}. Trianion $[4]^{3-}$ has a similar form to that of $[2]^{2-}$ with an additional contribution from an unpaired electron on a C_{60} moiety, whereas $[2]^{3-}$ appears as a monoradical based on fullerene due to spin-pairing of the electrons on PTCDI. The $[2]^{4-}$ and $[4]^{6-}$ ions are diamagnetic with all their electrons paired in fullerene and PTCDI orbitals. Anion $[4]^{4-}$ exists as a biradical with the two unpaired electrons of fullerene non-interacting and spin-pairing of the electrons in the PTCDI core. These results are completely consistent with the results from optical spectroscopy and demonstrate a range of electron interactions for these compounds.

The thorough understanding of the electronic and optical properties of these acceptor–acceptor dyads and triads reveals the formation of a series of reduced states that are readily accessible allowing tuning of the optical properties and magnetic states of these molecules. The results are of significance not only for the photochemical and chemical properties of the species reported but are crucial for further development of applications in photovoltaics and quantum information processing devices. Our studies continue to pursue these goals.

Experimental Section

Details of and information relating to all synthetic procedures are given in supporting information. Elemental analyses (CHN) were performed by the University of Nottingham, School of Chemistry Microanalytical Service on a Perkin–Elmer 240B instrument. Infra-red spectra were measured as solutions using a Nicolet Avatar 380 FT-IR spectrometer over the range 400–4000 cm^{-1}. ^{1}H and ^{13}C NMR spectra were obtained using a Bruker DPX 300 spectrometer. Mass spectrometry was carried out using a FAB-LSIMS spectrometer and a MALDI-TOF spectrometer at the EPSRC National Mass Spectrometry Service Centre in Swansea. Further details of experimental techniques, electrochemical/spectroelectrochemical and EPR spectroscopic measurements, are given in Supporting Information.

Acknowledgements

[1] K. Domen, J. N. Kondo, H. Hara, T. Takata, *Bull. Chem. Soc. Jpn.* **2000**, *73*, 1307.

[2] G. Yu, J. Gao, J. Hummelen, C. F. Wudl, A. J. Heeger, *Science* **1995**, *270*, 1789.

[3] a) H. Kurreck, M. Huber, *Angew. Chem.* **1995**, *107*, 929; *Angew. Chem. Int. Ed. Engl.* **1995**, *34*, 849; b) H. A. Staab, A. Feurer, R. Hauck, *Angew. Chem.* **1994**, *106*, 2542; *Angew. Chem. Int. Ed. Engl.* **1995**, *33*, 2428; c) M. R. Roest, J. W. Verhoeven, W. Schiddeboon, M. Warman, J. M. Lawson, M. N. Paddon-Row, *J. Am. Chem. Soc.* **1996**, *118*, 1762; d) D. Gust, T. A. Moore, A. L. Moore, *Pure Appl. Chem.* **1998**, *70*, 2189; e) D. Gust, T. A. Moore, A. L. Moore, *Acc. Chem. Res.* **1993**, *26*, 198; f) M. R. Wasielewski, *Chem. Rev.* **1992**, *92*, 435; g) M. N. Paddon-Row, *Acc. Chem. Res.* **1994**, *27*, 18; h) A. J. Bard, M. A. Fox, *Acc. Chem. Res.* **1995**, *28*, 141; i) T. J. Meyer, *Acc. Chem. Res.* **1989**, *22*, 163; j) P. Piotrowiak, *Chem. Soc. Rev.* **1999**, *28*, 143; k) J. L. Delgado, P.-A. Bouit, S. Filippone, M. Á. Herranz, N. Martín, *Chem. Commun.* **2010**, *46*, 4853.

[4] B. M. Illescas, N. Martín, *C. R. Chim.* **2006**, *9*, 1038.

[5] L. Bogani, W. Wernsdorfer, *Nature Mater.* **2008**, *7*, 179.

[6] W. Y. Kim, K. S. Kim, *Acc. Chem. Res.* **2010**, *43*, 111.

[7] S. C. Benjamin, A. Ardavan, G. A. D. Briggs, D. A. Britz, D. Gunlycke, J. Jefferson, M. A. G. Jones, D. F. Leigh, B. W. Lovett, A. N. Khlobystov, S. A. Lyon, J. J. L. Morton, K. Porfyrakis, M. R. Sambrook, A. M. Tyryshkin, *J. Phys.: Condens. Matter* **2006**, *18*, S867.

[8] M. Eiermann, R. C. Haddon, B. Knight, Q. C. Li, M. Maggini, N. Martín, T. Ohno, M. Prato, T. Suzuki, F. Wudl, *Angew. Chem.* **1995**, *107*, 1733; *Angew. Chem. Int. Ed. Engl.* **1995**, *34*, 1591.

[9] T. Ohno, N. Martín, B. Knight, F. Wudl, T. Suzuki, H. Yu, *J. Org. Chem.* **1996**, *61*, 1306.

[10] B. Knight, N. Martín, T. Ohno, E. Ortí, C. Rovira, J. Veciana, J. Vidal-Gancedo, P. Viruela, R. Viruela, F. Wudl, *J. Am. Chem. Soc.* **1997**, *119*, 9871.

[11] J. Baffreau, S. Leroy-Lhez, N. Vân Anh, R. M. Williams, P. Hudhomme, *Chem. Eur. J.* **2008**, *14*, 4974.

[12] R. Gómez, J. L. Segura, N. Martin, *Org. Lett.* **2005**, *7*, 717.

[13] J. Hua, F. Meng, F. Ding, F. Li, H. Tian, *J. Mater. Chem.* **2004**, *14*, 1849.

[14] S. Xiao, Y. Li, Y. Li, J. Zhuang, N. Wang, H. Liu, B. Ning, Y. Liu, F. Lu, L. Fan, C. Yang, Y. Li, D. Zhu, *J. Phys. Chem. B* **2004**, *108*, 16677.

[15] L. Schmidt-Mende, A. Fechtenkötter, K. Müllen, E. Moons, R. H. Friend, J. D. MacKenzie, *Science* **2001**, *293*, 1119.

[16] H. Quante, P. Schlichting, U. Rohr, Y. Geerts, K, Müllen, *Macromol. Chem. Phys.* **1996**, *197*, 4029.

[17] N. Martín, L. Sánchez, B, Illescas, I. Pérez, *Chem. Rev.* **1998**, *98*, 2527.

[18] H. Imahori, Y. Sakata, *Adv. Mater.* **1997**, *9*, 537.

[19] S. Fukuzumi, K. Ohkubo, H. Imahori, D. M. Guldi, *Chem. Eur. J.* **2003**, *9*, 1585.

[20] B. Maennig, J. Drechsel, D. Gebeyehu, P. Simon, F. Kozlowski, A. Werner, F. Li, S. Grundmann, S. Sonntag, M. Koch, K. Leo, M. Pfeiffer, H. Hoppe, D. Meissner, N. S. Sariciftci, I. Riedel, V. Dyakonov, J. Parisi, *Appl. Phys. A* **2004**, *79*, 1.

[21] B. E. Hardin, E. T. Hoke, P. B. Armstrong, J. H. Yum, P. Comte, T. Torres, J. M. J. Frechet, M. K. Nazeeruddin, M. Graetzel, M. D. McGehee, *Nat. Photonics* **2009**, *3*, 406; S. Ferrere, A. Zaban, B. A. Gregg, *J. Phys. Chem. B* **1997**, *101*, 4490.

[22] Y. Shibano, T. Umeyama, Y. Matano, N. Y. Tkachenko, H. Lemmetyinen, H. Imahori, *Org. Lett.* **2006**, *8*, 4425.

[23] H. Langhals, S. Demmig, H. Huber, *Spectrochim. Acta, Part A* **1988**, *44*, 1189.

[24] J. Fan, Y. Wang, A. J. Blake, C. Wilson, E. S. Davies, A. N. Khlobystov, M. Schroder, *Angew. Chem.* **2007**, *119*, 8159; *Angew. Chem. Int. Ed.* **2007**, *46*, 8013.

[25] H. Langhals, S. Kirner, *Eur. J. Org. Chem.* **2000**, 365.

[26] N. Miyaura, A. Suzuki, *Chem. Rev.* **1995**, *95*, 2457.

[27] M. Maggini, G. Scorrano, M. Prato, *J. Am. Chem. Soc.* **1993**, *115*, 9798.

FULL PAPER

[28] F. Würthner, V. Stepanenko, Z. Chen, C. R. Saha-Möller, N. Kocher, D. Stalke, *J. Org. Chem.* **2004**, *69*, 7933.

[29] C.-C. Chao, M.-k. Leung, Y. O. Su, K.-Y. Chiu, T.-H. Lin, S.-J. Shieh, S.-C. Lin, *J. Org. Chem.* **2005**, *70*, 4323.

[30] F. Arena, F. Bullo, F. Conti, C. Corvaja, M. Maggini, M. Prato, G. Scorrano, *J. Am. Chem. Soc.* **1997**, *119*, 789.